Vol. 42 No. 1 Journal of the Communications Research Laboratory March 1995
Printed in Tokyo, Japan pp. 111 - 119

THE HIRAISO RADIO SPECTROGRAPH (HiRAS) FOR MONITORING SOLAR RADIO BURSTS

By
Tetsuro KONDO, Takeshi ISOBE, Seiji IGI, Shin'ichi WATARI, and Munetoshi TOKUMARU

(Received on November 11, 1994)

ABSTRACT

A wideband radio spectrograph for monitoring solar radio emissions (receiving 25–2500 MHz) was newly installed at Hiraiso Solar Terrestrial Research Center in 1993. The spectrograph consists of three different frequency band antennas. Spectrum data from each antenna is combined to form a composite dynamic spectrogram. A data processing method based on the selection of minimum-data has been developed to remove man-made interference, such as radio and television signals, from raw spectrum-data. It has been successfully applied to actual observations and has served to improve the signal-to-noise ratio of solar burst emission spectrogram.

Keywords: sun, radio spectrograph, dynamic spectrogram

1. Introduction

The Hiraiso Solar Terrestrial Research Center has been monitoring solar radio emissions in order to predict significant disturbances in the solar-terrestrial environment for more than 40 years. These observations were made at fixed frequencies until 1988, when an initial spectrograph (70–500 MHz) with a 10 m antenna was installed. The solar radio-observation system at Hiraiso was renovated in 1993. By adding two antennas, the 70–500 MHz frequency range of the spectrograph was expanded about five times to 25–2500 MHz, making it sufficient to monitor the coronal radio emissions associated with flares. The frequency coverage of the new Hiraiso Radio Spectrograph (HiRAS) is now as wide as that of Culgoora radio spectrograph in Australia[1] which has been the widest frequency coverage (Fig. 1). Routine observations of the sun using the HiRAS began late in May 1993. Daily operation is fully automated, i.e., the antennas automatically track the sun from sunrise to sunset, and the data acquired by the spectrograph is processed by a workstation to produce a composite dynamic spectrogram. At the frequencies that HiRAS monitors, radio signals from the sun are always contaminated by artificial signals such as radio and TV broadcasts, especially at frequencies lower than 1 GHz. This contamination is thought to be worsening year by year as social activities progress. In order to make meaningful observations, we have developed software that effectively removes interference from raw spectrum data. This data processing method is being successfully applied to actual observation data, and solar-burst spectrogram quality has been significantly improved in terms of signal-to-noise ratio. This improvement has considerably increased the HiRAS ability to monitor solar radio bursts.

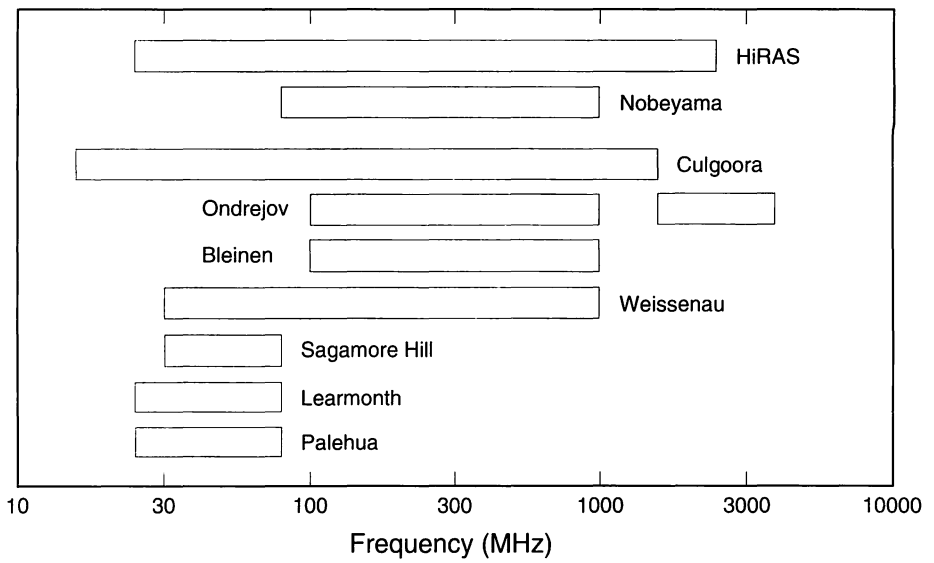

Fig. 1 A schematic representation of frequency coverage of major solar radio spectrographs: HiRAS and Nobeyama (Japan), Culgoora and Learmonth (Australia), Ondrejov (Czechoslovakia), Bleien (Switzerland), Weissenau (Germany), Sagamore Hill (USA), and Palehua (Hawaii, USA).

2. Antennas and Receiving System

A schematic block diagram of the new radio spectrograph at Hiraiso is shown in Fig. 2. The HiRAS consists of three antennas, HiRAS-1, HiRAS-2, and HiRAS-3, of which the receiving frequency ranges are 25–70 MHz, 70–500 MHz and 500–2500 MHz, respectively, making total frequency coverage 25–2500 MHz. Each antenna receives two orthogonal linearly polarized components. These crossed linearly polarized signals are combined by a wideband 90° hybrid-combiner to obtain right- and left-handed circular polarizations. Both circularly polarized signals are then amplified with low-noise pre-amplifiers and fed to spectrum analyzers. Spectrum data from the analyzers is passed to a system control computer (HP9000/R362) through GPIB every 2 to 5 seconds and then transmitted to a workstation (HP9000/710) via Ethernet. This three different band data are combined there to make a composite spectrogram.

2.1 HiRAS-1 (25–70 MHz)

The HiRAS-1 is a spatially-crossed 13-element log-periodic antenna with a nominal frequency coverage of 25–70 MHz. The antenna is installed on a 15 m tower in an azimuth-elevation type mount. The half-power beam width (HPBW) is about 60°. Crossed linearly polarized signals are combined by a wideband 90° hybrid combiner to obtain right- and left-handed circular polarizations. Each component is passed through a 25–75 MHz band-pass filter to prevent saturation amplifier due to the presence of strong signals (especially in the lower frequency region) just beyond the receiving band. Both polarized signals are then fed to amplifiers having a 40 dB gain and a 4 dB noise figure, and are passed from there to spectrum analyzers (HP8590D).

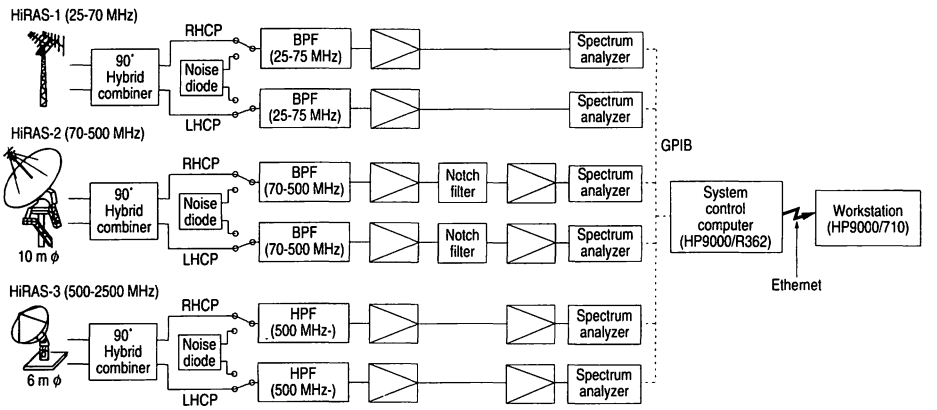

Fig. 2 A schematic block diagram of the Hiraiso radio spectrograph (HiRAS) displaying a data (signal) flow. The HiRAS consists of three antennas (HiRAS-1, HiRAS-2, and HiRAS-3) and covers a frequency range of 25 MHz to 2500 MHz. System control computer serves as both data acquisition and the HiRAS-3 antenna control. The HiRAS-1 and the HiRAS-2 have their own antenna control computers.

2.2 HiRAS-2 (70–500 MHz)

A 10 m parabolic dish with a crossed 20-element log-periodic feed antenna is utilized for the HiRAS-2, its frequency coverage is 70–500 MHz. The HiRAS-2 is mounted in an equatorial mount. The HPBWs at 70 MHz and 500 MHz are 29° and 4° respectively. Circularly polarized components are obtained from the two linearly polarized components using the same type of wideband 90° hybrid combiner used in the HiRAS-1. Better than 20 dB of isolation between right- and left-handed circular polarizations is obtained at all frequencies in the receiving band. Each polarization component is passed through a 70–500 MHz band pass filter and amplified using a low-noise 29 dB-gain amplifier with a noise rating of 1.7 dB. The amplified signal is then passed through a notch filter with two rejection frequencies (centered on 83.2 MHz and 280 MHz) to avoid saturation of the post amplifier by strong local FM-radio and telecommunicating signals. Both circular component signals are finally passed to spectrum analyzers (TR4135).

2.3 HiRAS-3 (500–2500 MHz)

The HiRAS-3 is a 6 m parabolic dish with a crossed 23-element log-periodic feed antenna. It has a frequency range of 500–2500 MHz and is mounted in an azimuth-elevation type mount. The HPBWs at 500 MHz and 2500 MHz are 6.5° and 1.4° respectively. The two linearly polarized components are combined by a wideband 90° combiner to make right- and left-handed circular polarizations as in the HiRAS-1 and the HiRAS-2. Each circular component is passed through a simple high-pass filter with a cutoff frequency of 500 MHz and is amplified using a low-noise amplifier (gain: 34 dB; noise figure: 1.2 dB). Both circular signals are then fed to spectrum analyzers (R4131D).

Characteristics of the three antennas, the settings of each spectrum analyzer, and overall characteristics of the HiRAS are summarized in Tables 1, 2, and 3. As an average sensitivity of the HiRAS is about 1 sfu (= 10^{-22}Wm^{-2}Hz^{-1}), the HiRAS can monitor all solar radio emissions except in the lower frequency region (< 70 MHz) when sun is quiet (see Fig. 3).

Table 1 Characteristics of HiRAS antennas

Characteristic	HiRAS-1	HiRAS-2	HiRAS-3
Diameter	–	10 m	6 m
Primary feed	Crossed 13-ele log-peri. antenna	Crossed 20-ele log-peri. antenna	Crossed 23-ele log-peri. antenna
Frequency range	25–70 MHz	70–500 MHz	500–2500 MHz
Antenna gain (dBi)	13	14.8 (70 MHz) 22.9 (200 MHz) 30.7 (500 MHz)	27.6 (500 MHz) 36.8 (1500 MHz) 40.8 (2500 MHz)
Beam width	60°	29° (70 MHz) 4° (500 MHz)	6.5° (500 MHz) 1.4° (2500 MHz)
Polarization	RHCP and LHCP	RHCP and LHCP	RHCP and LHCP
Mount type	Azimuth elevation	Equatorial	Azimuth elevation

Table 2 Spectrum analyzer settings

Setting	HiRAS-1 (HP8590D)	HiRAS-2 (TR4135)	HiRAS-3 (R4131D)
Resolution bandwidth	100 kHz	300 kHz	1 MHz
Video bandwidth	3 kHz	10 kHz	10 kHz
Sweep time	0.5 sec	0.5 sec	0.5 sec
Frequency range	20–70 MHz	50–550 MHz	500–2500 MHz
Detector mode	sample	sample	sample

Table 3 Overall characteristics of HiRAS

Frequency range	25–2500 MHz
Frequency resolution	501 points (on a log. scale)
Time resolution	3–4 sec
Polarization	RHCP and LHCP
Sensitivity	1 sfu (= 10^{-22}Wm^{-2}Hz^{-1})

3. Operation and Data Acquisition

Day-to-day observation is fully automated. Each antenna except for the HiRAS-3 has its own control computer and tracks the sun's position according to angles computed in real time. In the case of the HiRAS-3, the main system-control computer plays the role of the antenna control computer. Total tracking angle errors including both a calculation error and a mechanical error, are 10°, 0.1° and 0.1° for the HiRAS-1, the HiRAS-2, and the HiRAS-3, respectively. These values are below the minimum beam width of each antenna.

Spectrum data obtained by a total six spectrum analyzers is acquired by a system control computer (HP9000/R362) via the GPIB and immediately transferred to a workstation (HP9000/710) via an Ethernet. The information is then stored on a hard-disk mass storage system. The time

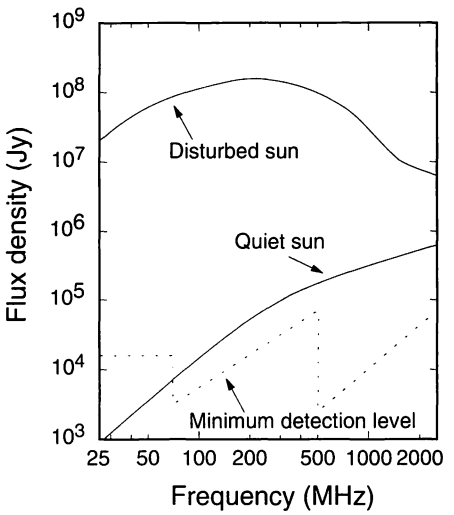

Fig. 3 Spectra of solar emissions in disturbed and quiet conditions and the minimum detection limit of the HiRAS (Jy = 10^{-26}Wm^{-2}Hz^{-1}).

resolution of observation is limited by data-acquisition capability of the system control computer. When the computer is devoted exclusively to data acquisition, it can gather data from the six analyzers every two seconds. In an actual operation, however, the period varies from 2 to 5 seconds because, as described above, the same computer also controls the movement of the HiRAS-3 antenna to track the sun, and this task sometimes interrupts data acquisition. This variation in sampling period is corrected during data processing to form a spectrogram.

4. Data Processing

Raw spectrum data gathered at Hiraiso is always contaminated by strong interference signals from local radio and television stations and other artificial sources. This interference degrades the quality of solar-burst spectrograms in terms of signal-to-noise ratio, resulting in less sensitivity in the detection of solar events. To improve the quality of these spectrogram a new data-processing algorithm was developed.

The upper panel of Fig. 4 shows an example of raw spectrum data gathered by HiRAS-2. The frequency dependence of the baseline and some of the dips are due to system characteristics. Many of the spikes seen in the spectrum stem from interference signals. Emissions from the sun can be seen as the baseline of the graph. The bandwidth of interferences is usually narrower than that of solar-burst signals. Therefore, it is possible to obtain the solar burst signal alone by reading the data points immediately next the interference spikes. This re-sampling may degrade the frequency resolution, however this is thought to be of negligible importance in solar radio observation, especially for the purpose of the emission-type classification described in the next section. To implement this idea we have developed software that reduces the number of samples in the frequency domain by about of a factor three, from 1803 points to 501 points, by re-sampling the data to select the minimum value in the frequency range corresponding to each new sample point. Spectrum data re-sampled this way, i.e., minimum-data selection, is shown in the lower panel of Fig. 4, from which it is clearly evident

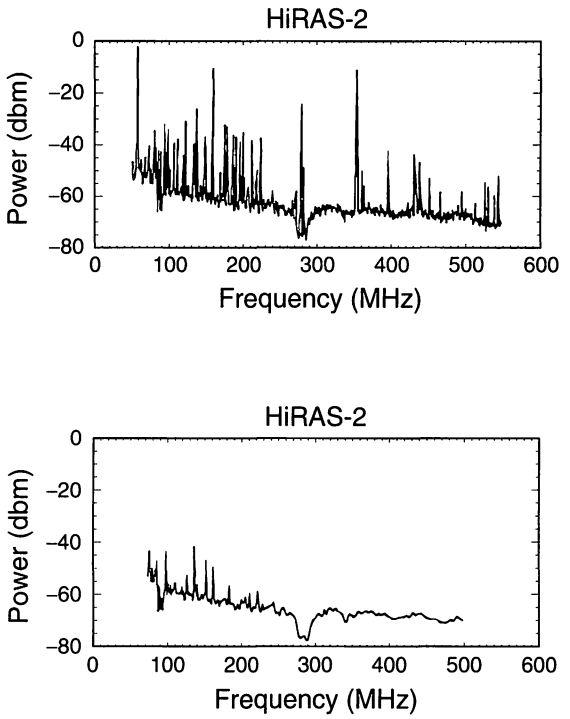

Fig. 4 An example of a raw spectrum gathered by the HiRAS-2 (upper panel) and the same spectrum data resampled to remove interference (lower panel). Many of the spikes in the raw spectrum are interference signals. Emissions from the sun can be seen as the baseline of the spectrum. Note that almost all interference seen in the raw spectrum has been successfully removed in the re-sampled data. The frequency dependence and some of the dips seen in the baseline are due to system characteristics.

that most of the interference seen in the raw spectrum data have been effectively removed. The new technique is thought to be acceptable for use in actual observation.

In addition to this processing, the solar-emission background level is subtracted from the spectrum data to increase the signal-to-noise ratio and thus to help separate burst events from the quiet-sun baseline. The background level is determined every three hours using the actual observation data for this period. To avoid the fluctuation of the received level due to a below horizon antenna image, the background measurement is limited to sun elevation angles higher than 10°.

This processing also serves to absorb differences in received signal level among the antennas. The upper panel of Fig. 5 shows a spectrogram from which interference has already been removed before background-level subtraction. The lower panel shows the spectrogram after all data processing, which includes both removal of interference and subtraction of background-signal level. It is clear that these data processing method significantly improve the quality of spectrograms.

5. Observations

Solar radio bursts associated with intense flares are classified into major five types (i.e., types I, II, III, IV and V on the meter wavelength band) on the basis of spectrogram appearance [2][3]. All five

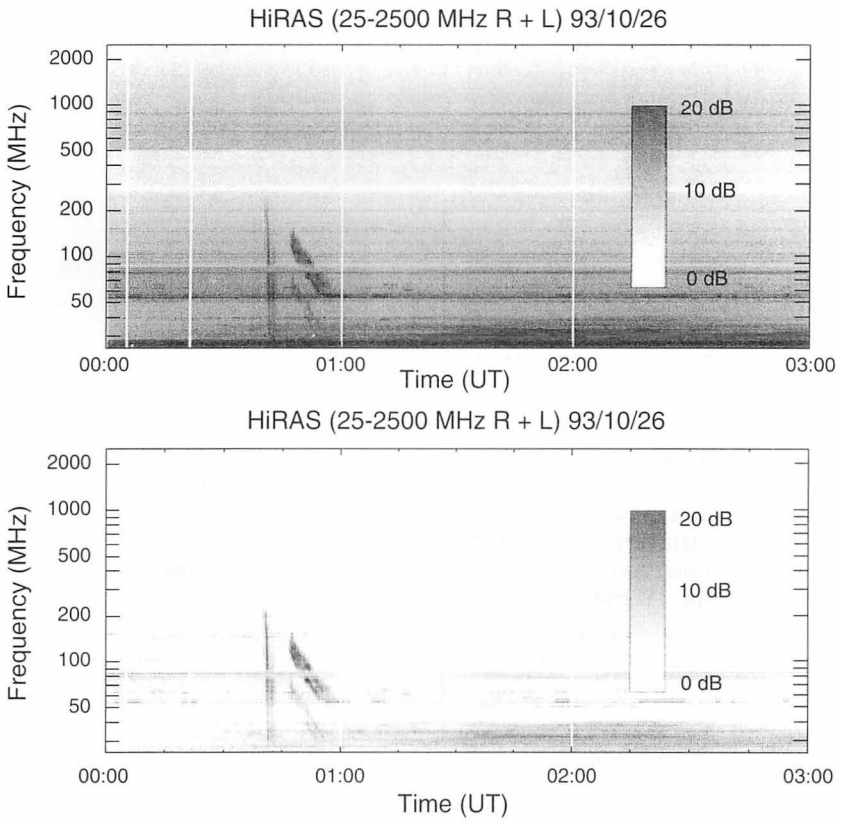

Fig. 5 The upper panel is a spectrogram after interference has been removed using the re-sampling method. The lower panel is a spectrogram which has been processed further, i.e., the background-signal level is subtracted from the data. Note that the signal-to-noise ratio of the spectrogram is significantly better in the lower panel. (This observation was made on Oct. 26, 1993. Type III emission occurred at 00:40, followed by type II emission starting at 00:47)

types have been observed by the HiRAS since May, 1993. Some examples are shown in Figs. 5 and 6. Figure 5 shows type III and II bursts observed on Oct. 27, 1993. Figure 6 shows type II and IV emissions associated with the large flare (M4.0/3B) which occurred on Feb. 20, 1994. This flare caused a geomagnetic storm starting in 32 hours. As this example demonstrated, the probability of occurrence of a geomagnetic storm becomes high when type II and IV emissions are both observed[4]. Hence, it is important for the prediction of a geomagnetic conditions to know the emission type associated with a flare. Furthermore, the speed of the plasmoid launched by the flare or coronal mass ejection (CME) event is also significant in estimating the time of its arrival at earth (i.e., the onset time of geomagnetic disturbance). The frequency-drift rate of type II bursts provides information about such speed, and an objective estimation method is now being developed for precise prediction—a principal purpose of the HiRAS's observations. The relationship between estimated shock speed and storm onset time is also being investigated.

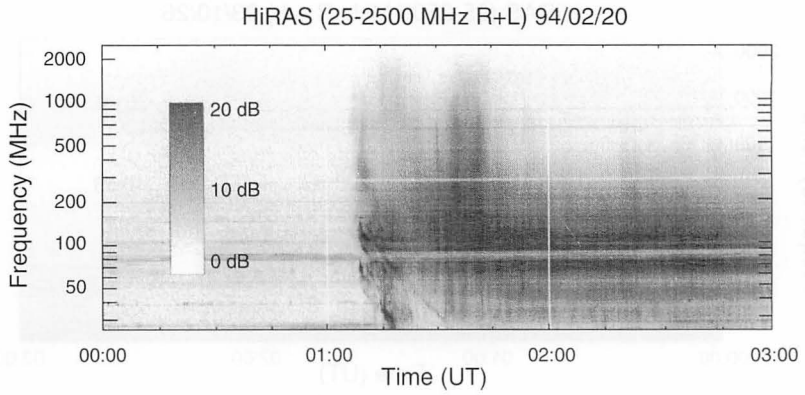

Fig. 6 Type II and IV emissions associated with an intense flare event which occurred on Feb. 20, 1994. The two gaps seen at 83 MHz and 280 MHz are due to the notch filter installed in the front end portion of the HiRAS-2. Type II emission can be seen as the negative frequency-drift structure starting at 01:10 with a lower edge frequency of about 50 MHz. Wide band continua seen in the frequency range below about 1000 MHz starting at the same time is type IV emission.

6. Concluding Remarks

Conditions for radio observations of weak natural signals becomes worse year by year due to the increase of artificial noise, especially at the one meter and longer wavelength bands. Under this negative conditions we have successfully improved the quality of observation by adopting a minimum-data selection technique for data processing. This improvement makes it easy to detect solar bursts and to classify them into five major types according to their appearance on the spectrograms. Among these five types, the co-occurrence of types II and IV becomes an important index in the prediction of the geomagnetic storms caused by flares or CME events. For these purposes, we plan to develop software to automatically extract and classify solar bursts from spectrograms using pattern-recognition techniques. In addition, shock speed has to be estimated when type II bursts occur. The HiRAS, with the help of such data processing techniques, will continue to contribute to increasing geomagnetic storm-prediction accuracy.

7. Acknowledgements

The authors would like to acknowledge the many people of Nihon Tsusinki Company and Toyo corporation who constructed the new Hiraiso radio spectrograph.

References

(1) R.G. Luckhurst and N.P. Prestage, "The new Culgoora radio-spectrograph," Technical Report of IPS Radio and Space Services, IPS-TR-93-03, 1993.

(2) M.R. Kundu, Solar Radio Astronomy, New York: Interscience Publ., 1965.
(3) D.E. Gary, "Radio observations during Max '91 campaign 1," MAX '91 Workshop #3: MAX '91/SMM Solar Flares: Observations and Theory, Colorado, pp. 1–10, 1990.
(4) G.J. Nelson and D.B. Melrose, "Type II bursts," in Solar Radiophysics, edited by D.J. McLean and N.R. Labrum, Cambridge Univ. Press, Ch. 13, pp. 332–359, 1985.